Relative Raman scattering cross sections of aqueous glucose

Michael DeFord[a], Richard Vanfleet*[a], Robert Davis[a], and Shintaro Pang[b]

[a]Department of Physics and Astronomy, Brigham Young University, Provo, USA
[b]Department of Nutrition, Dietetics, and Food Science, Brigham Young University, Provo, USA

ABSTRACT

Raman spectroscopy is a promising label-free approach for noninvasive glucose sensing, but quantitative system design requires accurate knowledge of how strongly individual glucose bands scatter light. We report experimentally measured relative Raman scattering cross sections for several aqueous glucose bands in the fingerprint region ($300 - 1500\ cm^{-1}$). Measurements were performed using a Raman microscope under fixed optical conditions, with neat liquid cyclohexane as a reference standard. A custom dual-reservoir sample holder enabled alternating reference and sample measurements to improve repeatability. Relative cross sections were measured using both 532 nm and 785 nm excitation. The excitation-wavelength dependence of the cross sections was then modeled using these measurements combined with literature values at 514.5 nm. For the four bands considered in this work ($444\ cm^{-1}$, $516\ cm^{-1}$, $1066\ cm^{-1}$, $1124\ cm^{-1}$), our cross section values range from 0.62×10^{-30} to $0.76 \times 10^{-30}\ cm^2 molecule^{-1} sr^{-1}$ for 785 nm excitation, and 4.1×10^{-30} to $4.6 \times 10^{-30}\ cm^2 molecule^{-1} sr^{-1}$ for 532 nm excitation. These values match well with the existing literature and expected wavelength dependence, and the resulting wavelength-dependence models can provide quantitative inputs for designing compact Raman glucose sensing systems.

Keywords: Raman spectroscopy, Raman scattering cross section, quantitative Raman spectroscopy, glucose sensing, optical biosensing, cyclohexane

1. INTRODUCTION

Blood glucose sensing is critical for diabetes management and other healthcare needs. Fingerstick, port, and implant solutions all come with significant costs, risks, and discomfort. As a result, a reliable method of noninvasive glucose sensing has long been sought after by the medical community.[1] Raman spectroscopy has been proposed as a potential solution due to its label-free molecular specificity.

Designing a device that uses Raman scattering to detect glucose noninvasively is a complex engineering challenge. A key part of that challenge lies in selecting an excitation wavelength that balances the weak Raman signal against interference from fluorescence and losses from water absorption and tissue scattering, among other things. Quantifying the Raman scattering cross section of glucose across physiologically relevant excitation wavelengths is crucial in that design process. However, the Raman scattering cross section of aqueous glucose has only been reported for a single excitation wavelength, 514.5 nm.[2,3] This is insufficient to model the wavelength dependence of the cross section.

In this work, we report a method for relative cross-section measurement, aqueous glucose cross-section measurements at two additional excitation wavelengths, and model the excitation-wavelength dependence for use in device design.

2. METHODS

We measured the relative Raman scattering cross section of $1M$ aqueous glucose by comparison to the known cross section of cyclohexane. We recorded polarized Raman spectra of glucose and cyclohexane under identical conditions, and fit peak areas to calculate the glucose cross section. The resulting cross sections were combined with literature values, and the excitation-wavelength dependence of the cross section was modeled using the single A-term Albrecht equation.[4]

*Corresponding Author. Email: richard.vanfleet@byu.edu

Enhanced Spectroscopies and Nanoimaging 2026, edited by Prabhat Verma, Yung Doug Suh,
Proc. of SPIE Vol. 14197, 1419709 · 2026 Published by SPIE
0277-786X · doi: 10.1117/12.3113961

2.1 Analyte Preparation

$1M$ aqueous glucose was prepared in 25 mL batches through the following process. First, the mass of dry glucose (Fisher Chemical, anhydrous) required to produce 25 mL of $1M$ solution, 4.504 grams, was precisely measured out using a calibrated Mettler AE 140 scale. The glucose was dissolved in 15 mL of type 1 ultrapure water and diluted to a final volume of 25 mL with additional ultrapure water. Neat liquid cyclohexane (J.T.Baker, HPLC/UHPLC-grade, 99.5+% purity) was used for the reference analyte.

2.2 Dual Reservoir Sample Holder

To enable consistent and repeatable measurements of both analytes, we designed a simple dual-reservoir sample holder (shown in Fig. 1). It consists of two small aluminum plates with holes for focusing and data collection. There is a slot in the bottom plate that accepts a standard 75 $mm \times 25\ mm \times 1\ mm$ quartz microscope slide (Ted Pella, Inc.). The reservoirs are formed by centering FFKM O-rings (Z1028-309, Marco Sealing Solutions) on the slide above each hole, filling one with each analyte, then covering each with a 0.25 mm thick quartz coverslip (Ted Pella, Inc.). The top plate compresses everything together with screws around the perimeter, sealing the reservoirs. Additionally, a PTFE washer (McMaster-Carr) is held in place under the center hole by a 3D-printed clip to provide a reference for focusing the microscope at a consistent height. A polarizing film (Edmund Optics, details in Tab. 2) sits on top of a 3D-printed carriage that maintains polarizer alignment between scans.

The holder enables scans of both analytes under functionally identical conditions while minimizing non-analyte Raman signal, maintaining consistent focus, and restricting all necessary movement to the motorized microscope stage. Multiple alternating scans, or alternating analyte points within a single scan, can be performed without opening the system or touching the sample holder.

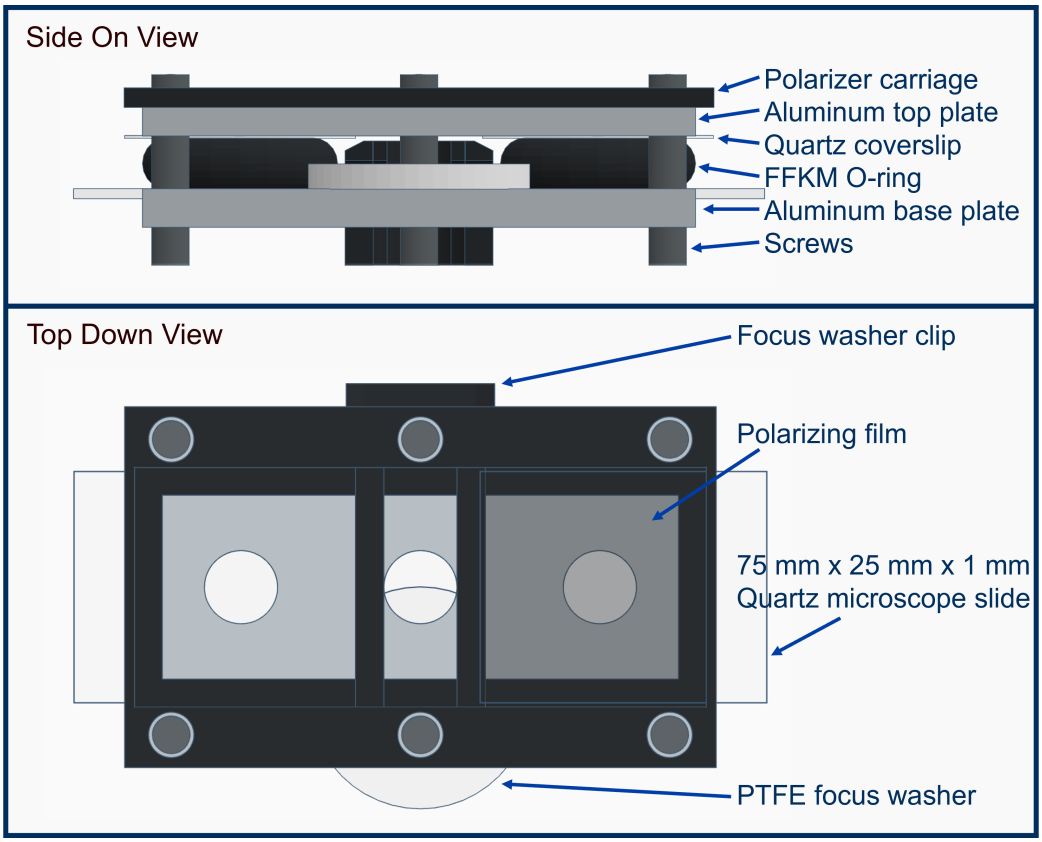


Figure 1. A schematic of the dual reservoir sample holder.

2.3 Raman Collection

All Raman spectra were collected with Thermo Scientific DXR2 and DXR3 Raman Microscopes using standard 10x objectives, running corresponding Thermo Scientific OMNIC software. Spectra were collected with both a 532 nm excitation laser and a 785 nm excitation laser. To address polarization mixing in the instrument optics, polarizing films were placed between the microscope objective and the analytes. This ensured that the excitation light reaching the analytes was fully polarized, and all the resulting collected Raman signal was also polarized. This cancels out any polarization mixing or bias in the collection optics during the relative cross-section calculation. Literature depolarization ratios[5,6] for the analytes are used to retrieve the total signal.

Raman microscope calibration and alignment were performed following the manufacturer's procedure before every round of data collection, and each time the lasers were swapped out. Scans were repeated if an automatic calibration occurred mid-scan, or between analytes, to ensure internal consistency. Tables 1 and 2 give the scan parameters and instrument details, respectively.

2.4 Data Processing

The spectra for all points within a scan were averaged together and then imported into PyRamanGUI, an open-source Raman analysis software.[7] Baseline subtraction was performed using the integrated Whitaker asymmetric least squares algorithm. Peak areas were then extracted by fitting curves to the spectra. For cyclohexane, a single Voigt curve was fit to the 801 cm^{-1} peak. For the aqueous glucose, a series of Lorentzians were simultaneously fit to the spectrum from 300 cm^{-1} to 1500 cm^{-1}. The 444 cm^{-1}, 516 cm^{-1}, 1066 cm^{-1}, and 1124 cm^{-1} glucose peaks were selected for analysis because their 514.5 nm Raman scattering cross-section values are documented in the literature.[2]

Each of these peaks is a convolution of multiple Raman modes and is best fit by multiple curves as shown in Fig. 2. The area under each peak of interest is the sum of the fitted Lorentzians that contribute to it.

2.5 Theory of Relative Cross-Section Measurement

Absolute Raman scattering cross-section measurements are the gold standard for quantitative Raman spectroscopy and design. However, absolute measurements are difficult and require careful control of experimental parameters and conditions to measure the cross section directly and accurately.[3] Alternatively, relative cross sections can be calculated by comparison to the few, well-characterized absolute measurements available in the literature.[2] Relative measurements taken under identical conditions remove from the equation many of the factors that would otherwise complicate the measurement.[8] These include instrumental factors, such as laser power, polarization biases, and collection and detector efficiencies, that would otherwise need to be carefully controlled and characterized.

Table 1. Raman microscope scanning parameters for data collection

Excitation Wavelength (nm)	532	785
Points per scan	25	25
Exposure duration (s)	5	5
Exposures per point	2	2
Laser power at objective (mW)	5	25
Pinhole Aperture Diameter (μm)	25	50

Table 2. Instruments and equipment used for data collection

Wavelength	532 nm	785 nm
Instrument	DXR3	DXR2
Laser Module	532 nm High Brightness	785 nm High Brightness
Grating Module	532 nm Full Range	785 nm Full Range
Polarizing Film	XP42-40	Broadband NIR

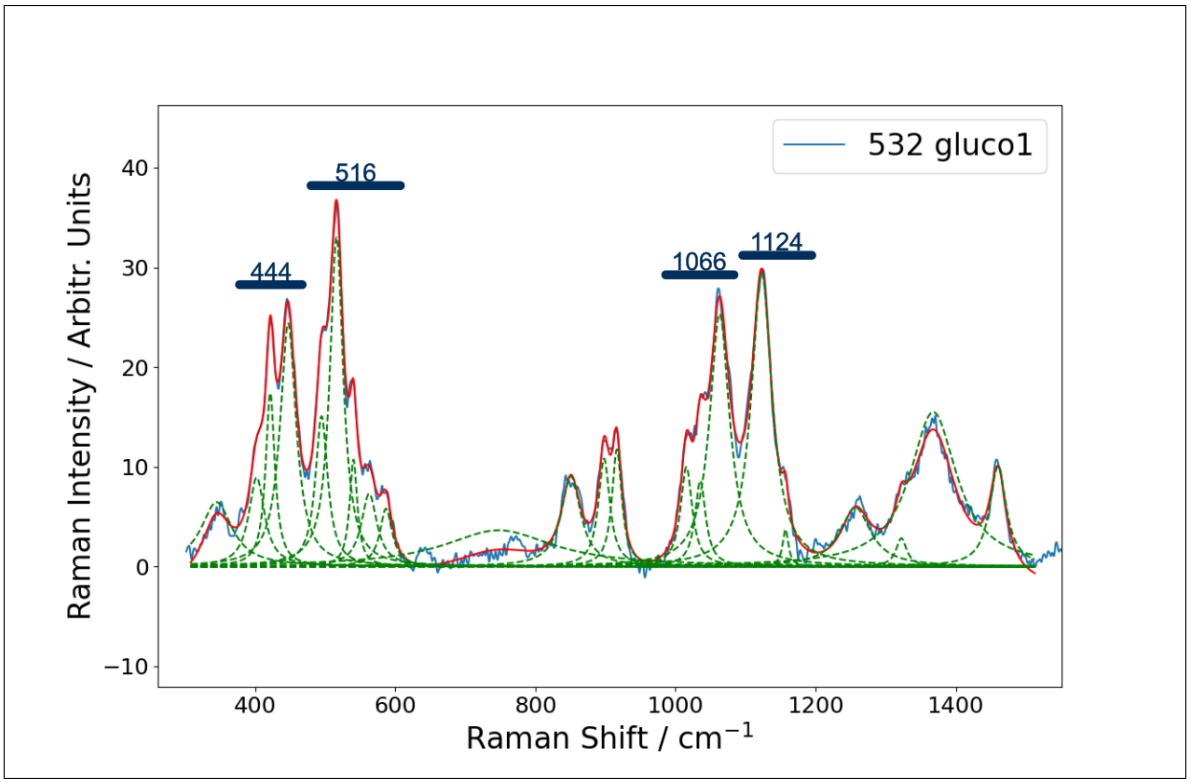


Figure 2. Polarized Raman spectrum of $1M$ aqueous glucose with example peak fitting. The light blue curve is the original data, the dashed green curves are the fitted Lorentzians, the red curve is the sum of the Lorentzians, and the navy blue bars mark the peaks of interest. The Lorentzians with centers within the width of each bar are summed to get the combined peak areas.

Relative cross sections are calculated by taking the product of a known cross section and a series of analyte property ratios. In the simplified general case, the primary factors are the peak area ratio, the number density ratio, and the ratio of the peak wavenumbers to the fourth power.[8] We have included an additional geometric factor, the analyte index of refraction ratio, to correct for the minor difference in interaction volume due to the focusing of the microscope objective through different analytes. This leads us to the following equation,

$$\frac{d\sigma_G}{d\Omega} = \frac{A_G}{A_C}\frac{\rho_{n,C}}{\rho_{n,G}}\frac{n_G}{n_C}\left(\frac{\nu_C}{\nu_G}\right)^4\frac{d\sigma_C}{d\Omega}, \tag{1}$$

where $d\sigma/d\Omega$ is the differential Raman scattering cross section, A is the peak area (including all polarizations), ρ_n is the molecular number density, n is the index of refraction, and ν is the wavenumber of the shifted peak. The subscripts G and C denote glucose and cyclohexane factors, respectively.

Our recorded spectra were linearly polarized parallel to the laser polarization, meaning all depolarized signals were attenuated. To recover the total signal, our parallel-polarized peak areas are modified by a depolarization factor

$$A = A_{\parallel}(1+\rho), \tag{2}$$

yielding

$$\frac{d\sigma_G}{d\Omega} = \frac{A_{\parallel,G}}{A_{\parallel,C}}\frac{(1+\rho_G)}{(1+\rho_C)}\frac{\rho_{n,C}}{\rho_{n,G}}\frac{n_G}{n_C}\left(\frac{\nu_C}{\nu_G}\right)^4\frac{d\sigma_C}{d\Omega}, \tag{3}$$

where ρ is the corresponding peak depolarization ratio, and $A_{\parallel}$ is the parallel-polarized peak area. Literature depolarization ratios come from Refs. 5 and 6 for cyclohexane and glucose, respectively.

Finally, reference values for the cyclohexane differential Raman scattering cross section were calculated using an experimental wavelength-dependence model from the literature.[9] This model gives values for the total Raman scattering cross section, which is converted to a differential cross section by[9]

$$\frac{d\sigma_C}{d\Omega} = \frac{3}{8\pi}\left(\frac{1+\rho_C}{1+2\rho_C}\right)\sigma_C, \tag{4}$$

where σ_C is the total cross section (including scattering in all directions and polarizations). This assumes that the acceptance angle of the microscope objective is narrow enough to approximate a backscattering geometry. Combining these factors yields

$$\frac{d\sigma_G}{d\Omega} = \frac{3}{8\pi}\frac{A_{\parallel,G}}{A_{\parallel,C}}\frac{\rho_{n,C}}{\rho_{n,G}}\frac{n_G}{n_C}\left(\frac{\nu_C}{\nu_G}\right)^4\left(\frac{1+\rho_G}{1+2\rho_C}\right)\sigma_C. \tag{5}$$

2.6 Wavelength Dependence Model

We modeled the preresonant excitation-wavelength dependence of the aqueous glucose Raman scattering cross section using the single A-term Albrecht equation[4,9]

$$\sigma(\nu_0) = K\left(\frac{\nu^2(\nu_e^2+\nu_0^2)}{(\nu_e^2-\nu_0^2)^2}\right)^2, \tag{6}$$

where K is the coupling strength fit parameter, ν is the peak wavenumber, ν_e is a fit parameter corresponding to a virtual resonant state, and ν_0 is the incident wavenumber. In accordance with the literature,[9] we fit the log_{10} of the measured cross sections to this model with nonlinear least squares to determine K and ν_e. This model is a valid approximation for excitation wavelengths far enough from resonance to be insensitive to the fine details of the resonance structure, and allows for interpolation and limited extrapolation.[4,9] Additionally, with this sparse dataset, other models with additional parameters would risk overfitting without meaningful improvements in confidence or accuracy.

3. RESULTS AND DISCUSSION

Our differential Raman scattering cross-section measurements and model fits are summarized in Tab. 3 along with the literature values with an excitation of 514.5 nm. Figure 3 shows the fitted curves with associated 80%, 90%, and 95% confidence intervals.

The uncertainty for each cross-section measurement was determined by propagating individual standard uncertainties, including experimental uncertainties, peak fitting, and cyclohexane calibration. Due to the overlapping curves used in fitting the glucose Raman spectra and potential correlations between parameters, the fitted peak area errors were combined using an area-weighted sum, rather than in quadrature, as a conservative

Table 3. The differential cross section for each peak by excitation wavelength, given in units of $10^{-30} cm^2 molecule^{-1} sr^{-1}$, and the model fit parameters with K also in units of $10^{-30} cm^2 molecule^{-1} sr^{-1}$ and ν_e in units of cm^{-1}. The large uncertainties in the fitting parameters are due to extremely high parameter correlation. Many pairs of parameter values would yield nearly identical fits.

Peaks	$\frac{d\sigma_G}{d\Omega}$ by Excitation Wavelength			Model Fitting Parameters	
$\Delta\nu$	785 nm	532 nm	514.5 nm	K	ν_e
444	0.76 ± 0.08	4.4 ± 0.5	6.1 ± 0.9	540 ± 780	67000 ± 20000
516	0.69 ± 0.06	4.1 ± 0.5	5.9 ± 1.0	400 ± 520	64000 ± 17000
1066	0.62 ± 0.06	4.1 ± 0.4	5.3 ± 0.5	630 ± 260	69000 ± 6000
1124	0.71 ± 0.05	4.6 ± 0.4	6.3 ± 0.8	590 ± 620	66000 ± 14000

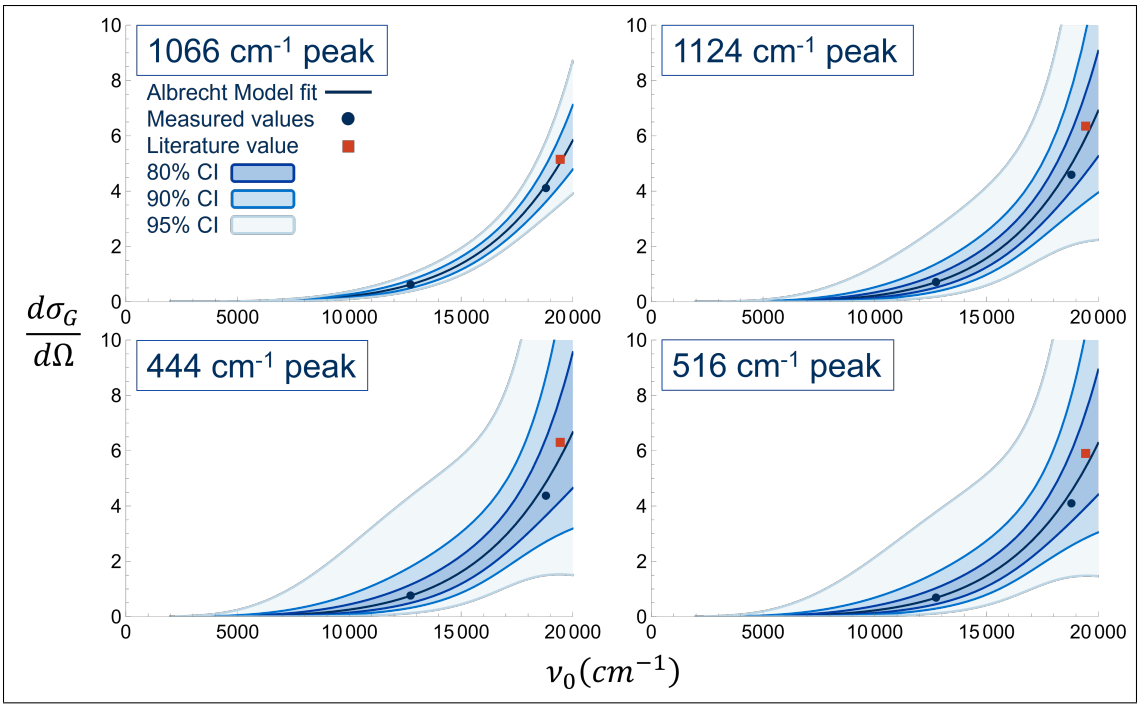


Figure 3. Fitted wavelength-dependence models for the differential Raman scattering cross section of each glucose peak. CI stands for confidence interval. The 80% CI for the 1066 cm^{-1} peak (top left) was removed for clarity. The literature values come from Ref. 2. Cross sections are plotted in units of $10^{-30} cm^2 molecule^{-1} sr^{-1}$ and the excitation wavenumber is plotted in cm^{-1}.

estimate of the total peak area uncertainties. The resulting combined standard uncertainties for the reported differential Raman scattering cross sections ranged from $7 - 12\%$.

The modeled fits in Fig. 3 show that our cross-section measurements align well with the established literature values. Being limited to only 3 data points, the models should be used cautiously, as evidenced by the width of the confidence intervals. This is especially true when extrapolating outside the measured excitation wavelengths,[9] though extrapolation to longer wavelengths is somewhat safer. Cross-section measurements at additional excitation wavelengths could be the subject of future work and massively improve the accuracy of the models. However, these models are sufficient to guide Raman device design with approximate values for physiologically relevant wavelengths.

Cross-section measurements at additional excitation wavelengths would also potentially reduce the uncertainty in the model fitting parameters. As they are, it is difficult to ascribe any physical meaning to them. Setting that aside to speculate, it is interesting to note that the ν_e values all fall between 64000-69000 cm^{-1}, which corresponds to 145-156 nm. Far-UV absorption spectra for glucose are not readily available in the literature, but sugars like glucose contain bonds with absorption peaks in that range,[10] which could be responsible for the preresonant enhancement. Additional work would be needed to confirm this.

4. CONCLUSION

We developed a straightforward method for relative differential Raman scattering cross-section measurements of transparent liquid analytes. We measured the differential Raman scattering cross sections of the 444 cm^{-1}, 516 cm^{-1}, 1066 cm^{-1}, and 1124 cm^{-1} peaks of $1M$ aqueous glucose, and modeled their excitation-wavelength dependence. These measurements align well with the established literature and provide approximate reference values that can be used to guide glucose-sensing Raman device design. Future work, such as further measurements with additional excitation wavelengths, would improve the accuracy and validity of this work.

ACKNOWLEDGMENTS

Special thanks to Built Brands, LLC, and their Lab Manager, Oumar Sanogo, for the use of their DXR2 Raman Microscope for the 785 *nm* scans.
This work was funded by Octavian Solutions.

REFERENCES

[1] Smith, J., [*The Pursuit of Noninvasive Glucose 9th Edition*], John Smith (12 2023).

[2] McAnally, M. O., Phelan, B. T., Young, R. M., Wasielewski, M. R., Schatz, G. C., and Van Duyne, R. P., "Quantitative determination of the differential raman scattering cross sections of glucose by femtosecond stimulated raman scattering," *Analytical Chemistry* **89**(13), 6931 – 6935 (2017).

[3] McCreery, R. L., [*Magnitude of Raman Scattering*], ch. 2, 15–33, John Wiley & Sons, Ltd (2000).

[4] Albrecht, A. and Hutley, M., "On the dependence of vibrational raman intensity on the wavelength of incident light," *The Journal of Chemical Physics* **55**(9), 4438 – 4443 (1971).

[5] Toleutaev, B., Tahara, T., and Hamaguchi, H., "Broadband (1000 cm-1) multiplex cars spectroscopy: Application to polarization sensitive and time-resolved measurements," *Applied Physics B Laser and Optics* **59**(4), 369 – 375 (1994).

[6] Mathlouthi, M. and Vinh Luu, D., "Laser-raman spectra of d-glucose and sucrose in aqueous solution," *Carbohydrate Research* **81**(2), 203 – 212 (1980).

[7] Brehm, S., Himcinschi, C., Kraus, J., and Kortus, J., "Pyramangui: Open-source graphical user interface for analyzing raman spectra," *SoftwareX* **23** (2023).

[8] McCreery, R. L. and Griffiths, P. R., [*Photometric Standards for Raman Spectroscopy*], John Wiley & Sons, Ltd (2006).

[9] Trulson, M. O. and Mathies, R. A., "Raman cross section measurements in the visible and ultraviolet using an integrating cavity: Application to benzene, cyclohexane, and cacodylate," *The Journal of Chemical Physics* **84**(4), 2068 – 2074 (1985).

[10] Uchiho, Y., Goto, Y., Kamahori, M., Aota, T., Morisaki, A., Hosen, Y., and Koda, K., "Far-ultraviolet absorbance detection of sugars and peptides by high-performance liquid chromatography," *Journal of Chromatography A* **1424**, 86 – 91 (2015).